IOP Publishing Science and Technology of Advanced Materials
Sci. Technol. Adv. Mater. **10** (2009) 013001 (18pp) doi:10.1088/1468-6996/10/1/013001

TOPICAL REVIEW

Hydrothermal growth of ZnO nanostructures

Sunandan Baruah and Joydeep Dutta

Centre of Excellence in Nanotechnology at the Asian Institute of Technology,
PO Box 4, Klong Luang, Pathumthani 12120, Thailand

E-mail: joy@ait.ac.th

Received 5 October 2008
Accepted for publication 14 November 2008
Published 13 January 2009
Online at stacks.iop.org/STAM/10/013001

Abstract
One-dimensional nanostructures exhibit interesting electronic and optical properties due to their low dimensionality leading to quantum confinement effects. ZnO has received lot of attention as a nanostructured material because of unique properties rendering it suitable for various applications. Amongst the different methods of synthesis of ZnO nanostructures, the hydrothermal method is attractive for its simplicity and environment friendly conditions. This review summarizes the conditions leading to the growth of different ZnO nanostructures using hydrothermal technique. Doping of ZnO nanostructures through hydrothermal method are also highlighted.

Keywords: ZnO, hydrothermal, nanostructures, synthesis, doping

(Some figures in this article are in colour only in the electronic version)

1. Introduction

Nanostructured ZnO materials have received considerable interest from scientists due to their remarkable performance in electronics, optics and photonics. As early as the 1960s, synthesis of ZnO thin films was an active field because of applications in sensors, transducers and as photocatalysts. In the last few decades, study of one-dimensional material has gained importance in nanoscience and nanotechnology. With reduction in size, novel electrical, mechanical, chemical and optical properties are introduced resulting from surface and quantum confinement effects.

ZnO is a significant technological material. The absence of a centre of symmetry in its wurtzite structure, along with large electromechanical coupling, results in strong piezoelectric and pyroelectric properties. ZnO is therefore widely used in mechanical actuators and piezoelectric sensors. In addition, ZnO is a wide band-gap (3.37 eV) compound semiconductor that is appropriate for short wavelength optoelectronic applications. The high exciton binding energy (60 meV) in ZnO crystal allows efficient excitonic emission at room temperature. ZnO is transparent to visible light and its conductivity can be increased through doping. ZnO nanostructures have a wide range of high technology applications like surface acoustic wave filters [1], photonic crystals [2], photodetectors [3], light emitting diodes [4], photodiodes [5], gas sensors [6], optical modulator waveguides [7], solar cells [8, 9] and varistors [10]. ZnO is also receiving a lot of attention because of its antibacterial property and its bactericidal efficacy has been reported to increase as the particle size decreases [11].

The discovery of carbon nanotubes by Iijima [12] in 1991 has initiated active research leading to the growth and characterization of one-dimensional nanowires of elemental and compound semiconductors such as Si [13], Ge [14], InP [15], GaAs [16] and ZnO [17–19]. Different nanostructures of ZnO have been reported such as nanowires and nanorods [20], nanocombs [21], nanorings [22], nanoloops and nanohelices [23], nanobows [24], nanobelts [25] and nanocages [26]. These structures have been successfully synthesized under explicit growth conditions [27].

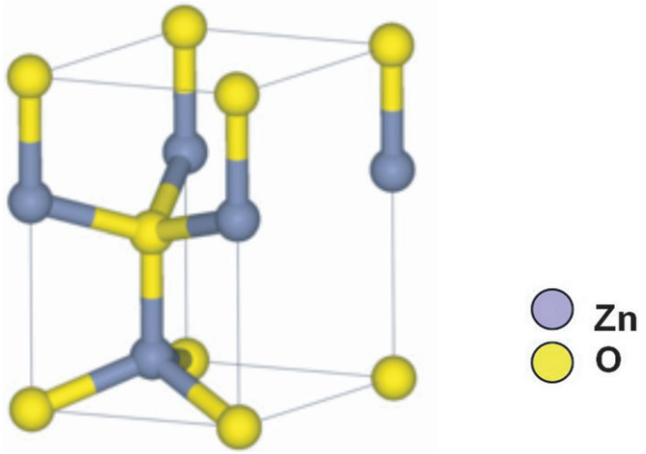

Figure 1. The wurtzite structure model of ZnO.

ZnO nanostructures can be grown either in solution or from gaseous phase. The gas phase synthesis methods are expensive and complicated. The solution phase synthesis is usually done in water. The hydrothermal process of growing ZnO nanostructures has gained immense popularity due to its simplicity and tolerable growth conditions. As synthesis is carried out in aqueous solution, the growth temperatures are less than the boiling point of water.

2. Zinc oxide: crystal structure

The ZnO crystal is hexagonal wurtzite and exhibits partial polar characteristics [27] with lattice parameters $a = 0.3296$ and $c = 0.52065$ nm.

The structure of ZnO can be described as a number of alternating planes composed of tetrahedrally coordinated O^{2-} and Zn^{2+} stacked alternately along the c-axis, as shown in figure 1. The tetrahedral coordination in ZnO results in piezoelectric and pyroelectric properties due to the absence of inversion symmetry. Another important characteristic of ZnO is polar surfaces. The most common polar surface is the basal plane (0001). One end of the basal polar plane terminates with partially positive Zn lattice sites and the other end terminates in partially negative oxygen lattice sites. The oppositely charged ions produce positively charged Zn-(0001) and negatively charged O-$(000\bar{1})$ surfaces, resulting in a normal dipole moment and spontaneous polarization along the c-axis as well as a variance in surface energy. To maintain a stable structure, the polar surfaces generally have facets or exhibit massive surface reconstructions, but ZnO $\pm$ (0001) surfaces are exceptions: they are atomically flat, stable and exhibit no reconstruction [1, 2]. Efforts to understand the superior stability of the ZnO $\pm$ (0001) polar surfaces are at the forefront of research in today's surface physics [3–6]. The other two most commonly observed facets for ZnO are $\{2\bar{1}\bar{1}0\}$ and $\{01\bar{1}0\}$, which are non-polar and have lower energy than the $\{0001\}$ facets.

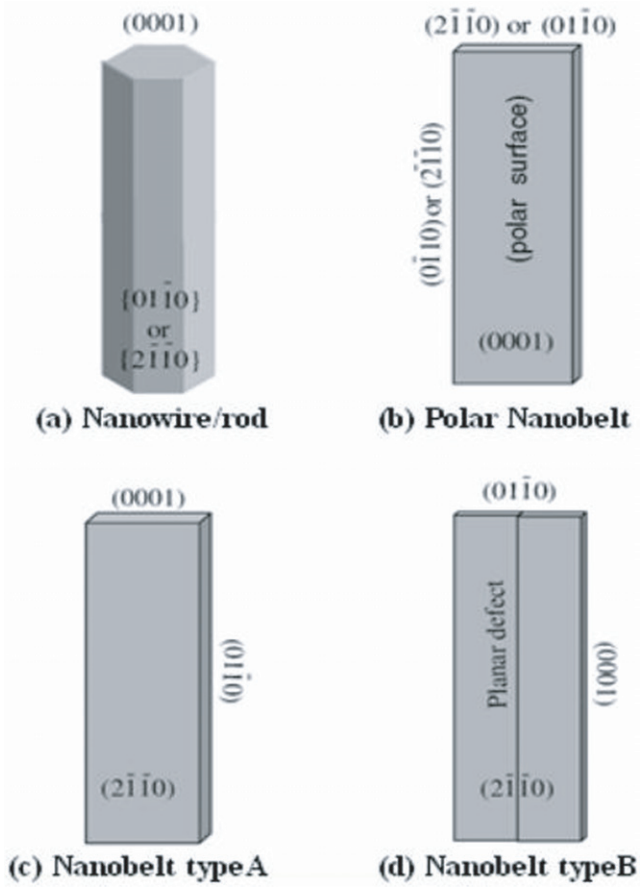

Figure 2. Growth morphologies of ZnO nanostructures with corresponding facets (reproduced with permission from [27] © 2004 IOP).

3. Zinc oxide: growth structures

ZnO exhibits a varied range of novel structures. These structures can be grown by tuning the growth rates along three fast growing directions: $\langle 2\bar{1}\bar{1}0\rangle$ ($\pm[\bar{1}2\bar{1}0]$, $\pm[2\bar{1}\bar{1}0]$, $\pm[\bar{1}\bar{1}20]$); $\langle 01\bar{1}0\rangle$ ($\pm[01\bar{1}0]$, $\pm[10\bar{1}0]$, $\pm[1\bar{1}00]$) and $\pm[0001]$. The relative surface activities of various growth facets under given conditions determine the surface morphology of the grown structure. Macroscopically, a crystal has different kinetic parameters for different crystal planes, which are emphasized under controlled growth conditions. Thus, after an initial period of nucleation and incubation, a crystallite will commonly develop into a three-dimensional object with well-defined, low-index crystallographic faces. Figures 2(a), (b) and (d) show a few typical growth morphologies of 1D nanostructures of ZnO. These structures tend to maximize the areas of the $\{2\bar{1}\bar{1}0\}$ and $\{01\bar{1}0\}$ facets because of the lower energy. The morphology shown in figure 2(b) is dominated by the polar surfaces, which can be grown by introducing planar defects parallel to the polar surfaces. Occasional planar defects and twins can be observed parallel to the (0001) plane, but dislocations are hardly seen [27].

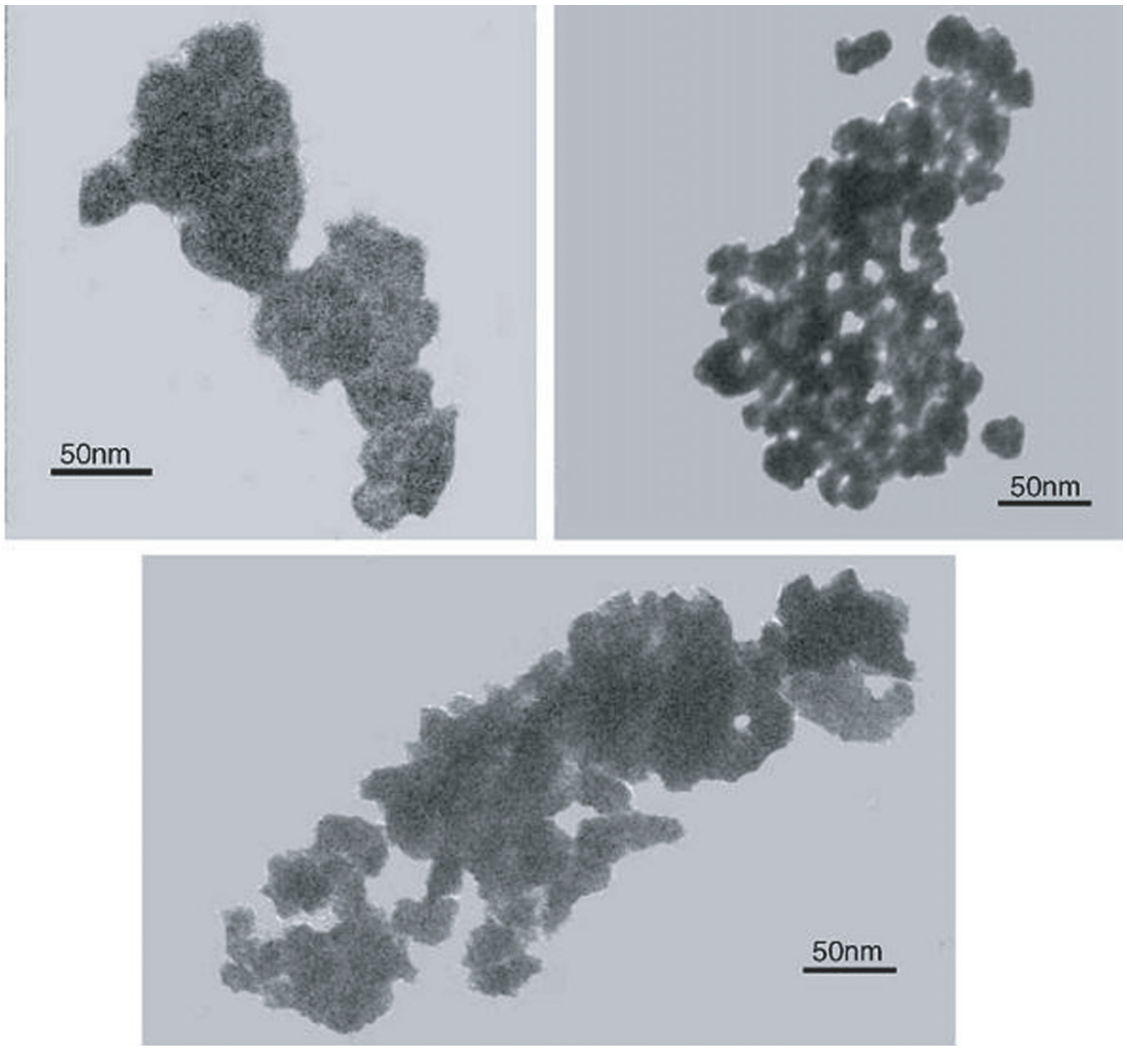

Figure 3. TEM images of the as synthesized ZnO nanoparticles using zinc nitrate hexahydrate in an autoclave at a temperature of 120 °C. (Reproduced with permission from [46] © 2006 Elsevier.)

Table 1. Partial charge distribution in ZAH derived precursor clusters. (Reproduced with permission for [28] © 2006 Springer)

Precursor clusters	δ_{Zn}	δ_{Ac}
$Zn(Ac)_2 \cdot 2H_2O$	0.471	−0.227
$Zn(Ac)_2$	0.469	−0.235
$Zn_4O(Ac)_6$	0.467	−0.245
$Zn_{10}O_4(Ac)_{12}$	0.465	−0.254
$Zn_5(OH)_8(Ac)_2 \cdot 2H_2O$	0.463	−0.269
$Zn_{10}O_4(Ac)_{12} \cdot H_2O \cdot 7EtOH$	0.429	−0.462
EtOZnAc	0.411	−0.567

4. Zinc oxide nanostructures—synthesis methods

The synthesis methods of different zinc oxide nanostructures can broadly be classified as follows:

a. *Solution phase synthesis*: In the solution phase synthesis, the growth process is carried out in a liquid. Normally aqueous solutions are used and the process is then referred to as hydrothermal growth process. Some of the solution phase synthesis processes are

1. Zinc Acetate Hydrate (ZAH) derived nano-colloidal sol-gel route [28].
2. ZAH in alcoholic solutions with sodium hydroxide (NaOH) or tetra methyl ammonium hydroxide (TMAH) [29–31].
3. Template assisted growth [32].
4. Spray pyrolysis for growth of thin films [33, 34].
5. Electrophoresis [35].

b. *Gas phase synthesis*: Gas phase synthesis uses gaseous environment in closed chambers. Normally the synthesis is carried out at high temperatures from 500 °C to 1500 °C. Some commonly used gas phase methods are

1. Vapour phase transport, which includes vapour solid (VS) and vapour liquid solid (VLS) growth [36–39].
2. Physical vapour deposition [40].
3. Chemical vapour deposition [41].
4. Metal organic chemical vapour deposition (MOCVD) [42].
5. Thermal oxidation of pure Zn and condensation [43].
6. Microwave assisted thermal decomposition [44].

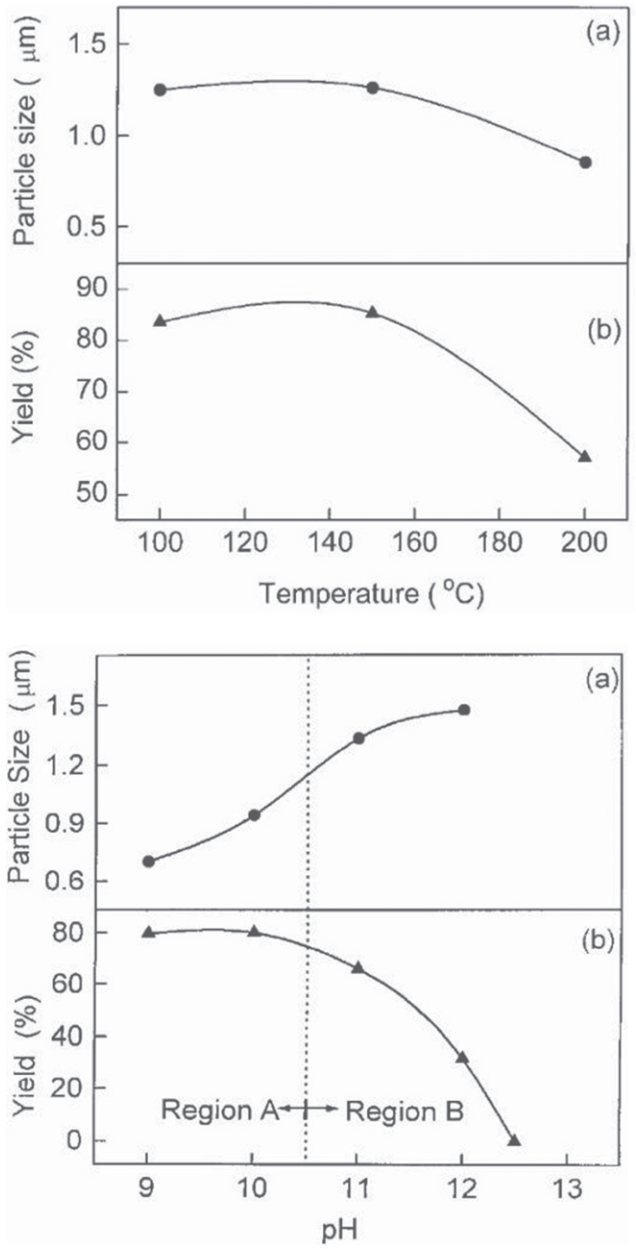

Figure 4. Variation in particle size and yield of the ZnO nano powders with growth temperature and pH of the growth solution. Region A: heterogeneous solution; region B: homogeneous solution. (Reproduced with permission from [47] © 2000 Elsevier.)

4.1. ZAH based sol-gel synthesis of ZnO nanostructures

The sol-gel method has gained a lot of popularity as it offers controlled consolidation, shape modulation and patterning of the nanostructures. Concentrated ethanolic zinc acetate hydrate (ZAH) suspension when refluxed and distilled forms a transparent sol. Small ZnO nanoparticles of dimensions around 5 nm can be grown under high concentration conditions by addition of hydroxides (e.g. LiOH, NaOH, etc) [28]. There are reports of modifications of the ZAH dehydration or dissolution and subsequent condensation for the growth of ZnO nanostructures [29–31].

Table 2. Morphologies obtained using different templates. (Reproduced with permission from [48] © 1999 Elsevier.)

	Particle properties	
Additives	Morphology	Size (nm)
Tributylamine	Rod-like	200–300
Triethylamine	Rod-like	100–300
Triethanolamie	Spindle-like	100–300
Diisopropylamine	Rod-like	200–400
Ammonium phosphate	Rod-like	200–500
1, 6-Hexadianol	Rod-like	300–700
Triethyldiethylnol	Rod-like	100–300
Isopropylamine	Rod or sheet-like	
Cyclohexylamine	Sheet-like	300–500
n-Butylamine	Sheet-like	200–400
Ammonium chloride	Sheet	50–200
Hexamethylenetetramine	Snow-flake like	20–50
Ethylene glycol	Ellipse	40–100
Ethanolamine	Polyhedron	50–200

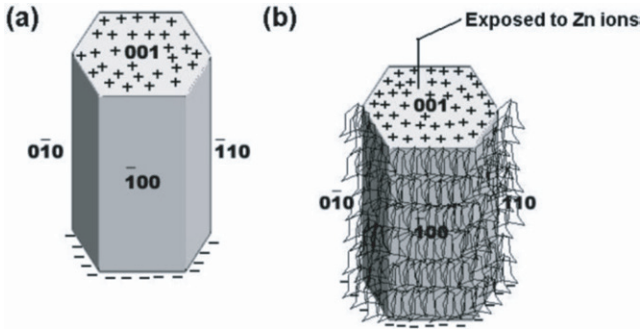

Figure 5. Attachment of hexamine to the non polar facets of the zincite crystal allows the growth of the crystal in the (0001) direction. (a) hexagonal ZnO crystal (b) possible attachment of hexamine on to the non polar facets leaving the polar face exposed allowing further crystal growth along the *c*-direction. (Reproduced with permission from [57] © 2006 Springer.)

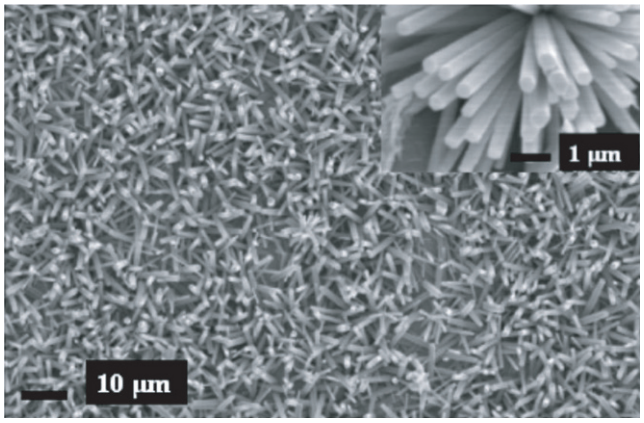

Figure 6. SEM image of ZnO nanorods grown using zinc nitrate and hexamine after seeding with ZnO nanoparticles. Inset: close up of the rods. (Reproduced with permission from authors [51].)

The search for primary clusters to serve as building blocks for various nanostructures has been going on for quite some time. The isolation and identification of primary clusters is an area of active research. The synthesis of the primary structures depend on various conditions like initial

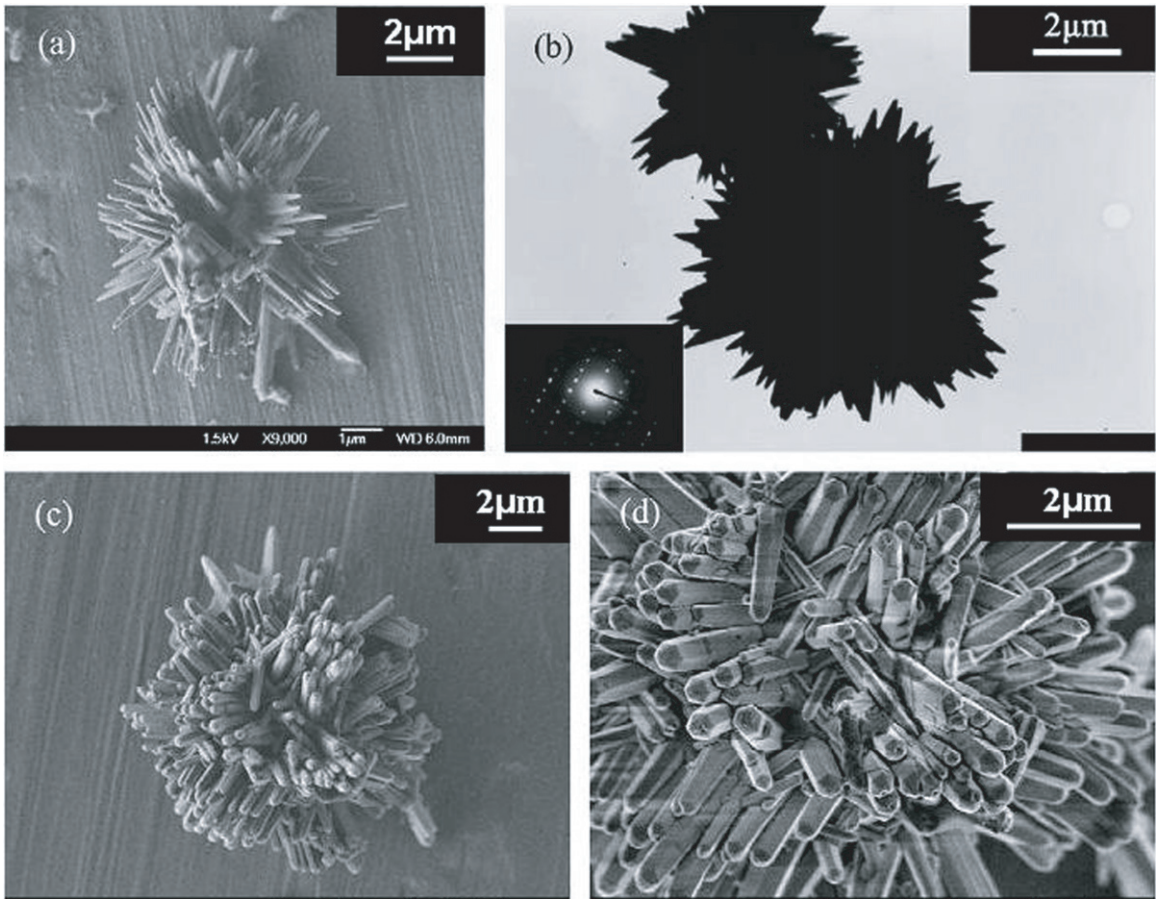

Figure 7. Images of ZnO homocentric bundles obtained in block copolymers systems: (a) SEM image: products in surfactant L64 (b) TEM image: products in L64. Inset: diffraction pattern. (c) and (d) SEM images: products in F68. (Reproduced with permission from [73] © 2007 Elsevier.)

concentration of the salt, the synthesis temperature, heating time as well as nature of the solvent. The ZnO clusters can be members of any of the three different families mentioned below [28]:

1. Tetrahedral oxy-acetate $Zn_4O(Ac)_6$.
2. Ethoxy acetate $(EtOZnAc)_n$.
3. Hydroxy-double salt $(Zn-HDS)Zn_5(OH)_8(Ac)_2(H_2O)_2$.

When $Zn(Ac)_2$ is heated in alcohol, the following reaction takes place initially

$$4Zn(Ac)_2 \cdot 2H_2O \xrightarrow{\text{heat}} Zn_4O(Ac)_6 + 7H_2O + 2HAc. \quad (1)$$

$Zn_4O(Ac)_6$ is also called *basic zinc acetate*. The by-products like H_2O, acetic acid etc, can be removed by distillation. ZAH forms a larger homologue $Zn_{10}O_4(Ac)_{12}$ when it is dehydrated in the presence of acetanhydride and refluxed in EtOH. Continuous refluxing of ZAH sols can result in ZnO nanoparticles [45]. $Zn_4O(Ac)_6$ can be considered as a well designed molecular model of ZnO.

Ethoxy acetates $(EtOZnAc)_n$ are formed in solutions having $Zn_{10}O_4(Ac)_{12}$ clusters. These species are formed gradually with time and after several weeks, large single crystals can be separated. The oxy-acetate clusters most probably generate intermediary zinc acetate monomers as shown by the following reactions:

$$4Zn_4O(Ac)_6 \longrightarrow Zn_{10}O_4(Ac)_{12} + 6Zn(Ac)_2, \quad (2)$$

$$Zn_4O(Ac)_6 + Zn_{10}O_4(Ac)_{12} \longrightarrow Zn_{13}O_5(Ac)_{16} + Zn(Ac)_2. \quad (3)$$

These $Zn(Ac)_2$ monomers can lead to formation of zinc ethoxy acetate $(EtOZnAc)_n$ crystals and acetic acid.

Hydroxy-double salt $(Zn\text{-}HDS)Zn_5(OH)_8(Ac)_2(H_2O)_2$ is formed by the titration of ZAH solutions with an aqueous solution of sodium hydroxide. Zn-HDS has been detected in precipitates of preheated alcoholic ZAH sols. At high temperatures and after prolonged refluxing, Zn-HDS can be easily transformed into ZnO nanoparticles.

Table 3. Difference reaction for growth of ZnO nanorods. Reproduced with permission from [78] © 2007 Elsevier.

Sample	NH_4OH (g)	Reaction time (h)
A_1	1.5	12
A_2	1.5	24
A_3	3.5	12
A_4	3.5	24

Table 4. Morphology and shape of difference ZnO nonostructures at varying pH. (Reproduced with permission from [82] © 2008 Elsevier.)

pH	Morphology		Shape
9.0	Coalescence of Zno	Coalescence	Budding flower
9.5	Nano-particles	↑	
10.0	Zno nanorod		Blossom
10.5	Separation sharp rods	Separation	Chestnut but or echinoid
11.0	Separation of thick rods	↓	Dense chestnut bur
11.5	Coalescence of rods		Gingko leaves
11.8	Archetype of thick rods	Coalescence	Dendelion

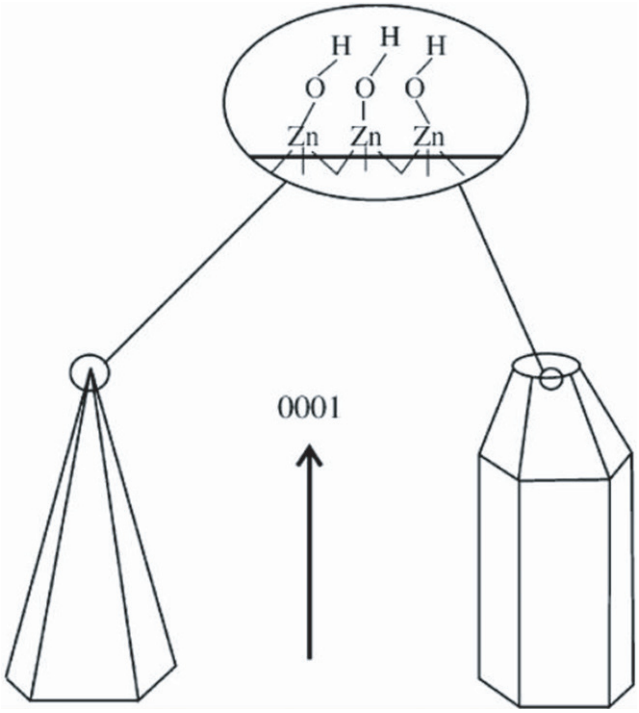

Figure 8. Growth habits of hexagonal prism- and pyramid-like ZnO crystals. (Reproduced with permission from [73] © 2007 Elsevier.)

The occurrence of hydroxy double salts during the growth of ZnO nanoparticles may be due to the following:

1. H_2O induced reorganization of the tetrahedral species (primary and secondary) formed during initial nucleation. Hydroxyl ions also play a role.

$$Zn_4O(Ac)_6 + Zn(Ac)_2 + 9H_2O \longrightarrow 2Zn_5(OH)_8(Ac)_2(H_2O)_2 + 6HAc. \quad (4)$$

$$Zn_{10}O_4(Ac)_{12} + 16H_2O \longrightarrow 2Zn_5(OH)_8(Ac)_2(H_2O)_2 + 8HAc. \quad (5)$$

$$Zn_{10}O_4(Ac)_{12} + 16H_2O + 8OH^- \longrightarrow 2Zn_5(OH)_8(Ac)_2(H_2O)_2 + 8Ac^-. \quad (6)$$

2. The continuous liberation of zinc acetate during the growth of the ZnO nanoparticles may be another reason for the growth of the hydroxy double salts.

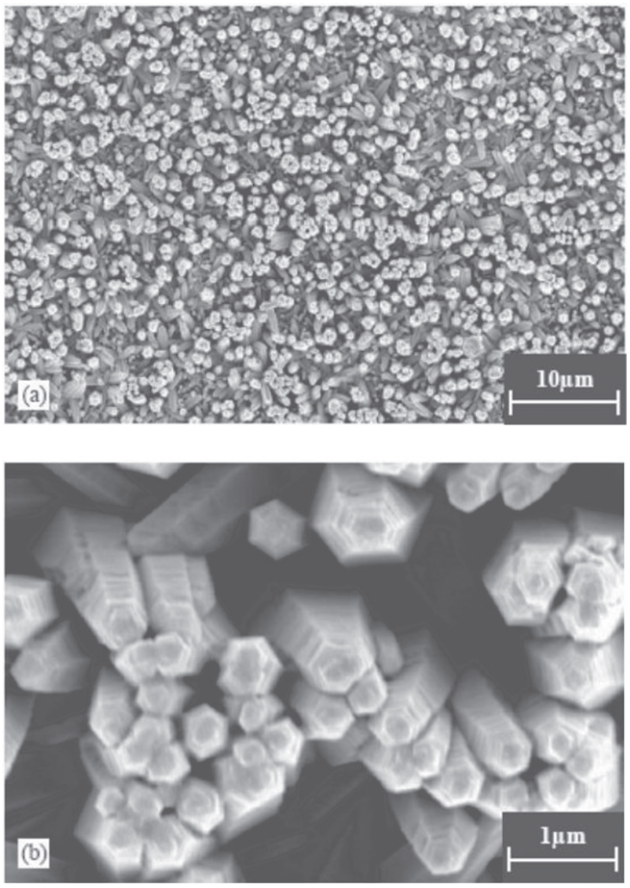

Figure 9. SEM images of the array of ZnO obelisk shaped nanorods grown on glass substrate. (Reproduced with permission from [75] © 2004 Elsevier.)

4.2. Stability of ZAH derived structures

Spanhel [28] carried out partial charge calculations using the Henry–Livage model. The partial charge values for the ZAH structures are shown in table 1.

It can be observed that the tetrahedral oxy-acetate clusters are slightly more stable than the zinc acetate hydrate. Further, the stability of $Zn_{10}O_4(Ac)_{12}$ precursor is strongly increased in the presence of H_2O and EtOH. Once a certain amount of water is present, there is a spontaneous formation of zinc hydroxy double salts (Zn-HDS). This is because of the higher stability of the Zn-HDS monomer with respect to the naked oxy-acetate clusters. As seen from the table 1, the most stable precursor cluster is the zinc ethoxy-acetate. An important point to note is that Zn^{2+} ions do not exist as free ions in alcoholic ZAH solutions as a strong chemical bond exists between Zn^{2+} ions and Ac ligands in all the compounds in table 1.

4.3. ZnO nanostructures through hydrothermal growth

4.3.1 Nanoparticles. Even though the organometallic synthesis of ZnO nanoparticles in alcoholic medium has received wider acceptance for reasons of faster nucleation and growth as compared to water, still scattered reports of hydrothermal synthesis in aqueous medium are available in

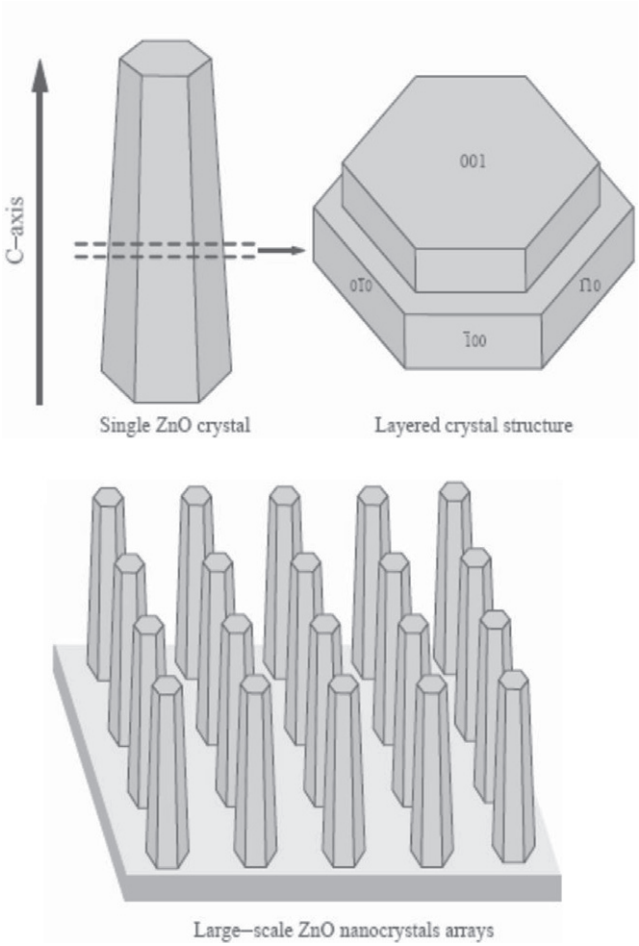

Figure 10. Illustration of the crystal structure of the obelisk shaped ZnO nanorods. (Reproduced with permission from [75] © 2004 Elsevier.)

the literature. Baruwati *et al* [46] have reported the aqueous synthesis of ZnO nanoparticles using zinc nitrate hexahydrate. Synthesis was carried out in an autoclave at a temperature of 120 °C after adjusting the pH to 7.5 using ammonium hydroxide. After washing, the particles were dried at 80 °C overnight to obtain the powder form. The as synthesized particles are shown in the transmission electron microscope (TEM) images in figure 3.

Lu *et al* [47] successfully prepared crystalline ZnO powder through a hydrothermal process using ammonia as the base source. With $Zn(NO_3)_2$ as the source of Zn^{2+} ions, growth was carried out at 100 °C, 150 °C and 200 °C for 2 h and the effect of growth temperature and pH was studied. Figure 4 shows the variation of particle size of the ZnO powder and its yield as functions of growth temperature and pH. With pH < 11 in region A of figure 4, the zinc hydroxide precursors are dissolved partially and the ZnO powder is nucleated in a heterogeneous system. On the other hand, in region B with pH $\geqslant$ 11, all zinc hydroxide precursors are dissolved and a clear solution is formed so that ZnO powder is nucleated in a homogeneous solution. Different nucleation states thus take place in regions A and B with higher probability of nucleation in the heterogeneous solution.

Chen *et al* [48] synthesized nanoparticles of different morphologies using $ZnCl_2$ and NaOH in a hydrothermal growth process using different organic compounds as template agents. A significant change in the morphology was observed as the synthesis temperature was increased with the particles changing from rod like to polyhedral. It was reported that the morphology also changed with the addition of different organic templates to the reaction mixture when the temperature was maintained at 160 °C. The various morphologies along with the templates used are listed in table 2.

A very simple procedure to prepare ZnO nanoparticles at a very high pH ∼ 14 using tetramethylammonium hydroxide (TMAH) as a precipitating agent was suggested by Musić *et al* [49]. Nanoparticles sized from 10 to 20 nm were precipitated at room temperature by adding TMAH to an ethanolic solution of zinc acetate dehydrate. Addition of water to the ethanolic solution prior to adding TMAH yielded ZnO snowflakes.

Vishwanathan and Gupta [50] have shown that supercritical water can also be a good reaction medium for the hydrothermal synthesis of ZnO nanoparticles. Spherical ZnO nanoparticles were synthesized by oxidation of zinc acetate in supercritical water in a continuous tubular reactor. Particle size and morphology can be controlled by varying conditions like temperature, pressure or the reaction atmosphere. Nanoparticles with diameters ranging between 39 and 320 nm were synthesized using this method.

The synthesis time has been significantly reduced through the use of microwave irradiation and the ZnO nanocrystallites thus formed were observed to be more defective than the ones synthesized over a few hours of hydrolysis [51]. Nanoparticles with inherent defects are capable of exhibiting visible light photocatalysis even without doping with transition metals, which is the normally followed method.

4.3.2 Nanowires and nanorods. Andres-Vergés *et al* [52] first reported the hydrothermal method of growing ZnO nanostructures. However, this could not instil much interest till Vayssieres *et al* [53] successfully used the method for the controlled fabrication of ZnO nanowires on glass and Si substrates by the thermal decomposition of methenamine and zinc nitrate. To initiate the growth from the substrate, a thin layer of ZnO nanoparticles was grown on the substrate. Methenamine, also known as hexamethylenetetramine (HMT) or hexamine is a highly water soluble, non-ionic tetradentate cyclic tertiary amine. Thermal degradation of HMT releases hydroxyl ions which react with Zn^{2+} ions to form ZnO [54]. This can be summarized in the following equations:

$$(CH_2)_6N_4 + 6H_2O \leftrightarrow 6HCHO + 4NH_3, \quad (7)$$

$$NH_3 + H_2O \leftrightarrow NH_4^+ + OH^-, \quad (8)$$

$$2OH^- + Zn^{2+} \rightarrow ZnO(s) + H_2O. \quad (9)$$

It is a general acceptance that the role of HMT is to supply the hydroxyl ions to drive the precipitation reaction [55]. Apart from that, some also opine that HMT acts as a buffer as the

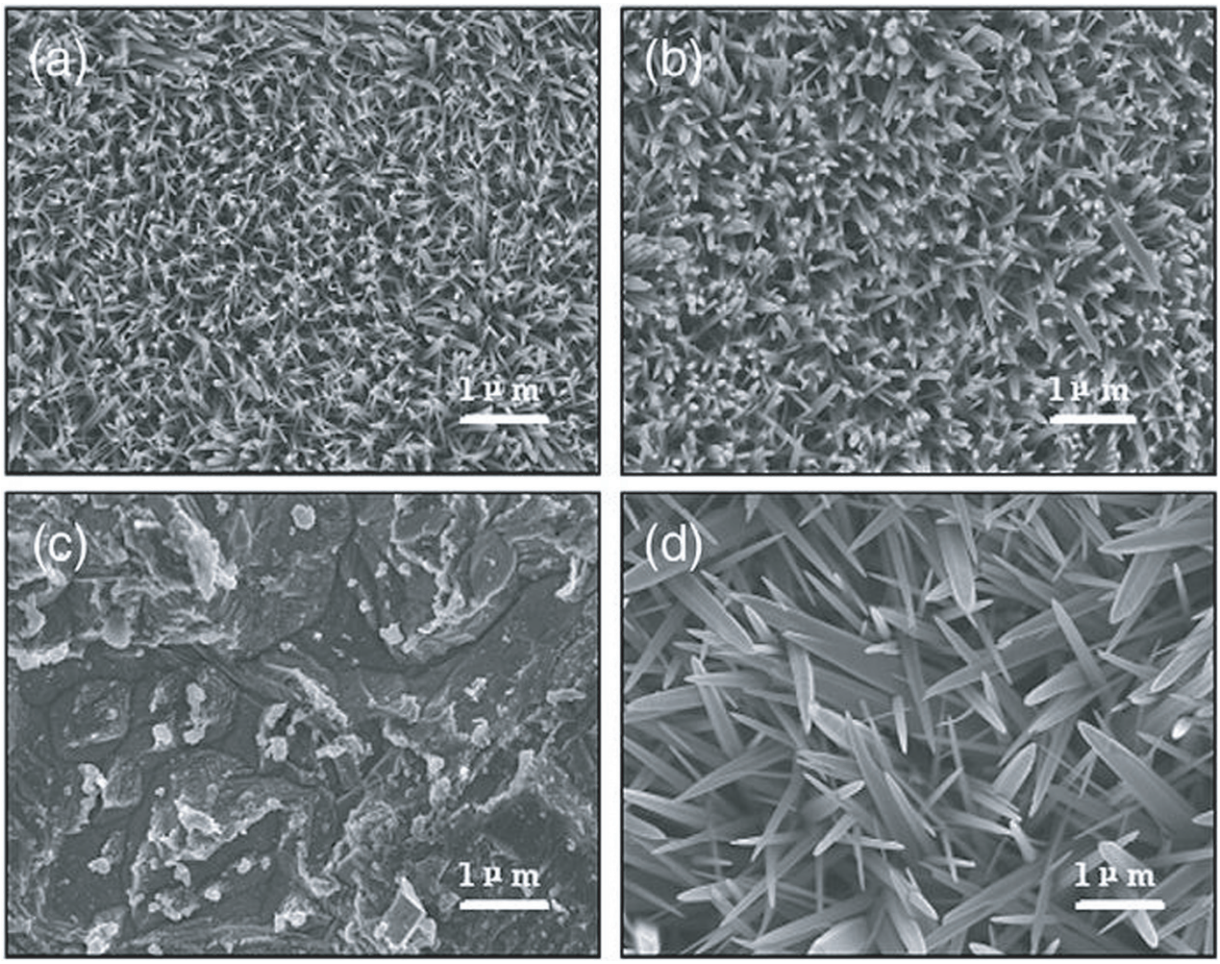

Figure 11. SEM images of the ZnO nanostructures on Zn foil with condition mentioned in table 3: (a) A_1 (b) A_2 (c) A_3 (d) A_4. (Reproduced with permission from [78] © 2007 Elsevier.)

rate of its hydrolysis decreases with increasing pH and vice versa [56]. Ashfold *et al* [55] have demonstrated that the rate of decomposition of HMT is independent of the reaction that yields ZnO indicating that HMT does act as a kinetic buffer. In oxide formation, the phase that is thermodynamically less stable will precipitate out faster [56]. In the initial growth stage, the pH and the concentration of Zn^{2+} ions is such that the ZnO growth will be through $Zn(OH)_2$. With the gradual increase in the pH and the decrease in the concentration of the Zn ions, $Zn(OH)_2$ becomes thermodynamically unstable and the $Zn(OH)_2$ formed on the substrate will start dissolving. Further growth of the nanostructures will have to be through direct deposition of ZnO [55].

The contribution of HMT in the growth process of ZnO nanowires has also been discussed by Sugunan *et al* [57] in a totally different approach. It was proposed that HMT, being a long chain polymer and a nonpolar chelating agent, will preferentially attach to the non polar facets of the zincite crystal, thereby cutting off the access of Zn^{2+} ions to them leaving only the polar (001) face for epitaxial growth. HMT therefore acts more like a shape-inducing polymer surfactant rather than as a buffer. Figure 5 shows the mechanism of attachment of hexamine on the nonpolar facets.

There is a lot of literature reporting investigation on the growth and properties of ZnO nanorods synthesized using zinc nitrate and HMT such as the effect of substrates and seed layers on the morphology of nanorods and nanotubes [58–60], growth on different substrates [20] and the control of aspect ratio through the addition of citrate anions [61]. Pal and Santiago [62] have managed to control the morphology of ZnO nanostructures by varying the amount of a soft surfactant, ethylenediamine and the pH of the reaction mixture of zinc acetate, sodium hydroxide and the surfactant. Homogenous growth was observed at a pH of 12 with inhomogeneity creeping in as the pH decreases. A 10% concentrated ethylenediamine gave higher aspect ratio than 5% concentration. Figure 6 shows scanning electron microscope (SEM) images of hydrothermally grown ZnO nanorods using zinc nitrate and hexamine.

ZnO nanowires and nanorods have been successfully synthesized using different surfactants and numerous reports are available. Tang *et al* [63] synthesized ZnO nanorods using zinc acetylacetonate $Zn(acac)_2 \cdot H_2O$ as a single source precursor and investigated the growth of the rods in the presence of four different surfactants: polyvinyl alcohol (PVA), polyethylene glycol (PEG), sodium dodecyl sulphate

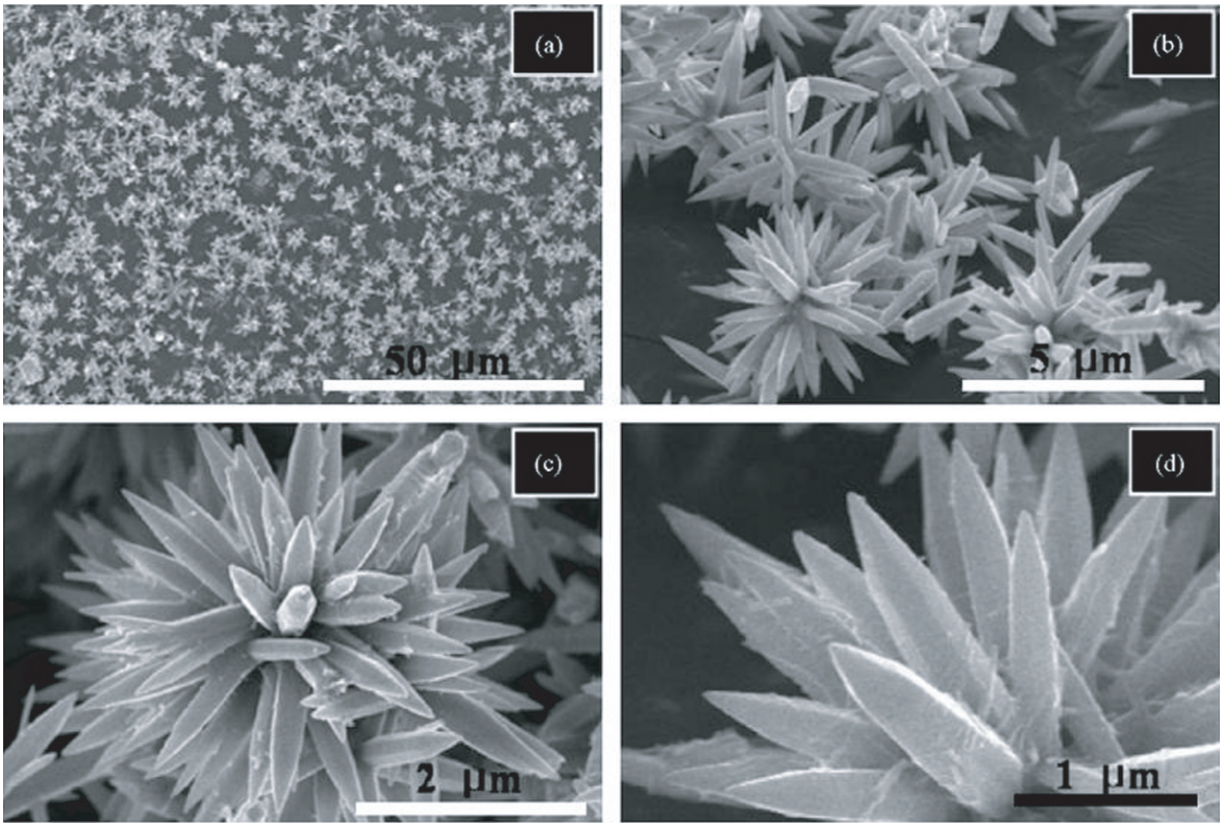

Figure 12. SEM images of the flower-like ZnO nanostructures at different magnifications. (Reproduced with permission from [79] © 2007 Elsevier.)

(SDS) and cetyltrimethyl ammonium bromide (CTAB). The use of PVA resulted in more regular and defect free rods than PEG, SDS and CTAB. Li *et al* [64] has reported the growth of tapered ZnO nanorods with diameter decreasing from 400 nm at the body to about 80 nm at the tip from CTAB assisted hydrothermal growth. Zinc acetate dehydrate was used as the precursor and the pH was adjusted to 13 using KOH. The use of carbamide $CO(NH_2)_2$ as a surfactant [65] in a hydrothermal growth with $ZnSO_4$ and NaOH yielded highly crystalline ZnO nanobelts. Chen *et al* [66] studied the effect of potassium iodide (KI) as a surfactant in the crystallization of ZnO nanorod clusters from a chemical bath containing zinc nitrate hexahydrate $Zn(NO_3)_2 \cdot 6H_2O$ and hydrazine hydrate $N_2H_4 \cdot H_2O$. They obtained step growth of hexagonal nanorod clusters, and this morphology is attributed to the presence of iodine ions in the growth bath. Stepped columns of ZnO were also observed using CTAB as the surfactant [67]. Experiments further showed that the source of Zn ions can also affect the morphology of the end product. Ni *et al* [67] obtained ZnO nanorods in place of stepped columns simply by changing the source of Zn ions from $Zn(Ac)_2$ to $ZnCl_2$ and keeping all other conditions same. This may be due to the change in pH of the growth bath.

Water soluble amphiphilic block copolymers, PEO-PPO-PEO, due to their unique properties are being used as templates for the ingenious morphologies of inorganic materials such as nanoparticles, mesoporous materials and hierarchically ordered oxides [68–72]. Zhang *et al* [73] managed to control the shape of bundles of ZnO nanostructures through a macromolecular surfactant (L64 and F68) assisted hydrothermal growth route. The bundles of ZnO nanostructures are shown in figure 7.

It was deduced that the nanobundle superstructures of ZnO result from a two-step mechanism in aqueous solutions with initial nucleation followed by the growth of the nanorods around these nuclei. Overall size and arm lengths are probably controlled by the growth velocity of ZnO particles and the micelle dimension of PEO–PPO–PEO copolymers. ZnO is a polar crystal, O^{2-} is in hexagonal closest packing, and each Zn^{2+} lies within a tetrahedral group of four oxygen ions [74]. Zn and O atoms are stacked alternatively along the *c*-axis and the top face (0001) consists of tetrahedral zinc having a terminal OH ligand as shown in figure 8. The formation of hexagonal prism and pyramid like ZnO crystals is attributed to the difference in the growth velocities of various crystal facets. The growth velocities under hydrothermal conditions along the different directions are known to follow the pattern $V(0001) > V(1011) > V(1010)$ [73]. The relative growth rate of these crystal faces will determine the final shape and aspect ratio of the ZnO nanostructures. The preferential growth along the (0001) polar direction proceeds unabated and the ZnO nanorods would appear in the end products. Although the chemical reaction is relatively simple, the growth process of ZnO nanobundles is quite complicated. It can be presumed that the faster the growth rate, the quicker the disappearance of the plane. The (0001) plane disappears due to its high growth velocity leading to the pointed shape at the end of the *c*-axis. As a consequence of the slow growth

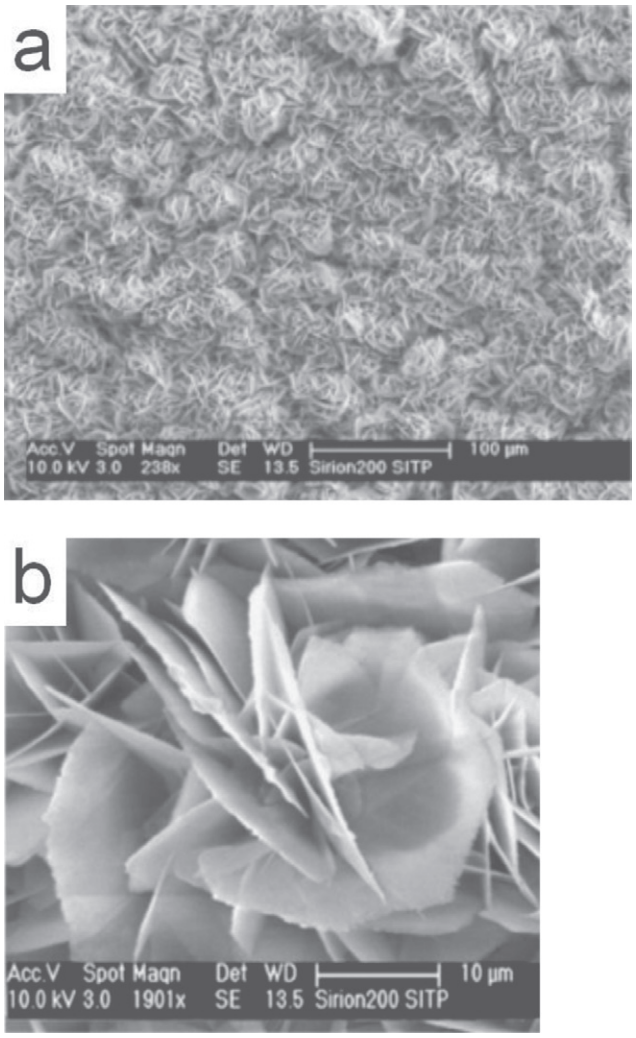

Figure 13. SEM images of ZnO nanoflowers synthesized using zinc chloride and ammonia. (Reproduced with permission from [80] © 2007 Elsevier.)

of the (1010) plane, the crystal remains to form the hexagonal prisms, while the (1011) plane corresponds to the formation of the hexagonal pyramid like tips.

Wang *et al* [75] has shown that it is possible to efficiently synthesize large two-dimensional arrays of obelisk shaped ZnO nanorods on quartz or glass substrates through a simple hydrothermal deposition method with zinc nitrate, ammonia and ammonium hydroxide as the precursors. The single-crystalline obelisk rods with diameters ranging between 300 and 400 nm and lengths of about 5 μm were grown in Teflon vessel at 95 °C for 30 min and the SEM images are shown in figure 9.

The mechanism for the formation of ZnO crystals using ammonia can be summarized in the following equations [76, 77].

$$NH_3 + H_2O \Leftrightarrow NH_3 \cdot H_2O \Leftrightarrow NH_4^+ + HO^-, \quad (10)$$

$$Zn^{2+} + NH_3 \rightarrow Zn(NH_3)_4{}^{2+}, \quad (11)$$

$$Zn(NH_3)_4{}^{2+} + OH^- \rightarrow ZnO. \quad (12)$$

or ZnO may also form from the complex ion $Zn(OH)_4{}^{2+}$ as below:

$$Zn^{2+} + OH^- \rightarrow Zn(OH)_4{}^{2-}, \quad (13)$$

$$ZnOH_4{}^{2+} \rightarrow ZnO. \quad (14)$$

The complex ions $Zn(NH_3)_4{}^{2+}$ and $Zn(OH)_4{}^{2-}$ formed due to the mixing of zinc nitrate, ammonia and ammonium hydroxide, dehydrate to initiate heterogeneous nucleation of ZnO on the substrate. The possible formation of the obelisk-shaped single-crystalline rods is attributed to multiple layered structures as explained in figure 10.

The presence of Zn^{2+} containing salts is not a necessity for the growth of ZnO nanostructures through the hydrothermal growth method. Li *et al* [78] has successfully grown large scale arrays of ZnO nanorods on zinc foil without the assistance of any template, oxidant or coating of metal oxide layers, simply by dipping the foil into a 25% aqueous solution of ammonia (NH_4OH) and heating at a temperature 80 °C in a Teflon-lined stainless steel autoclave. Four different samples were prepared by varying the concentration of ammonia in a 80 ml growth bath and the growth duration as shown in table 3. The SEM images are shown in figure 11.

It was observed that the thickness, density and morphology of the ZnO nanorod arrays are affected by the alkalinity of the solution in the growth bath. The sharp tips of the nanorods are probably due to the concentration gradient of Zn^{2+} from the base to the tip. The increase in growth time only led to thicker rods with the lengths remaining almost comparable. With the increase in concentration of ammonia, no growth was observed till 12 h but a very dense growth of uneven pointed rods was observed when the growth duration was increased to 24 h.

4.3.3 Flower-like and cabbage-like nanostructures. Flower-like structures are very typical of ZnO and can be synthesized using simple hydrothermal methods. Wahab *et al* [79] has reported the growth of flower-like ZnO using hydrothermal method. The flowers, composed of hexagonal ZnO nanorods, were synthesized at a temperature of 90 °C using zinc acetate dehydrate and sodium hydroxide in aqueous solutions. The flowers, with nanorod petals as long as 2–4 μm, could be synthesized in just 30 min. SEM images of the nanoflowers are shown in figure 12. All the pointed nanorods emerged from a single centre thereby acquiring the spherical shape.

Flower-like ZnO nanostructures with nanosheet petals was synthesized by Shao *et al* [80] through a hydrothermal route using zinc chloride and ammonia as the reactants. The flowers, averaging in size of about 30 μm, are composed of sheets of thickness about 150–250 nm. SEM images (figure 13) reveal numerous well distributed nanostructures formed all over the copper plate substrate.

Li *et al* [81] has reported the growth of flower-like and cabbage-like nanostructures using CTAB as the surfactant in a hydrothermal growth process at temperatures of 120, 150 and 180 °C. They obtained flower-like micro and nanostructures consisting of ZnO nanorods at a temperature of 120 °C.

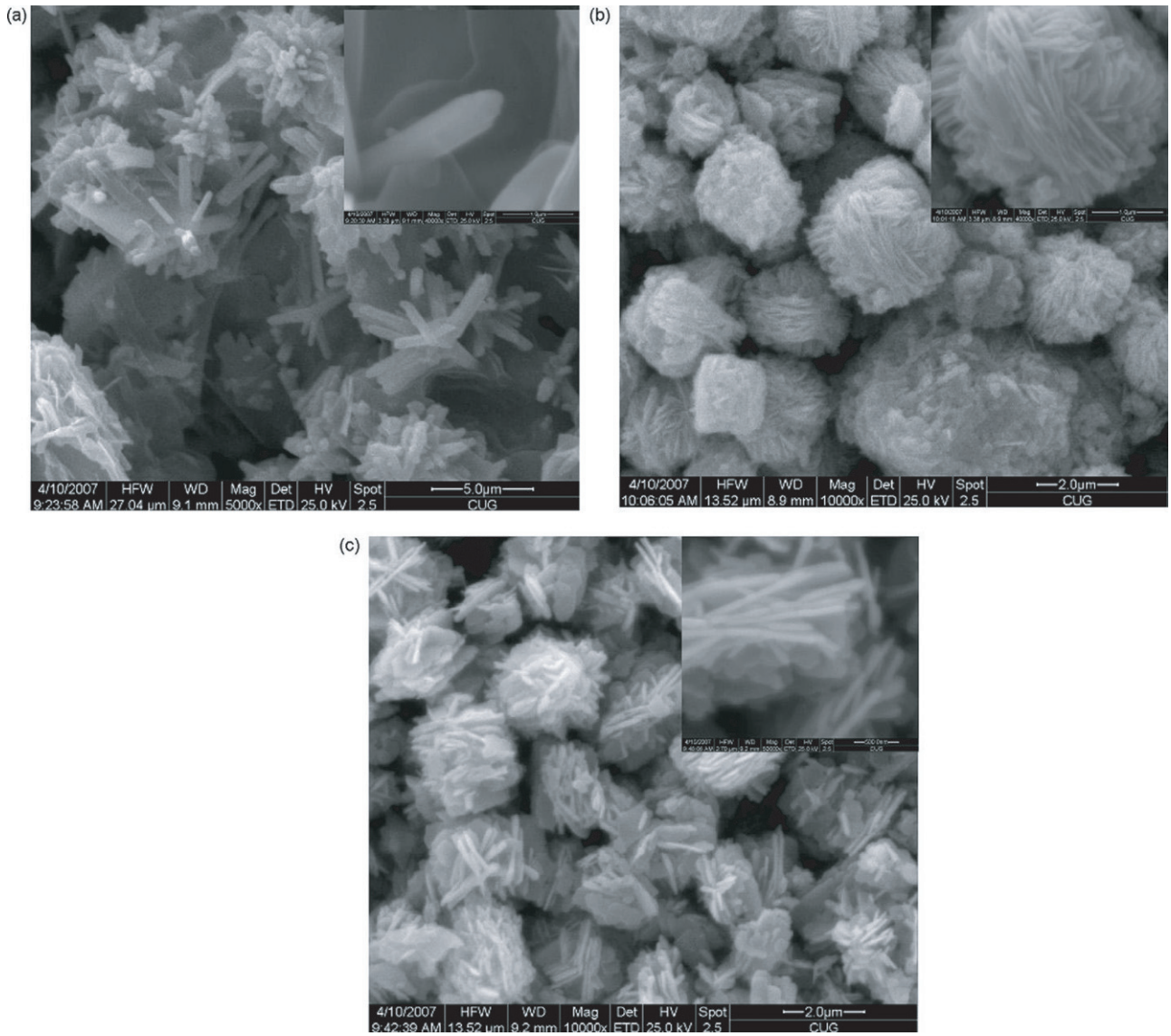

Figure 14. SEM images of as-synthesized ZnO micro and nanostructures prepared by CTAB-assisted hydrothermal growth at various temperatures (a) 120 °C (b) 150 °C and (c) 180 °C. Inset: magnified images. (Reproduced with permission from [81] © 2008 Elsevier.)

As the synthesis temperature was increased to 150 and 180 °C, cabbage-like structures were formed due to the repeated growth of two-dimensional ZnO nanosheets. The thickness of the nanosheets obtained at 150 °C was about 50 nm and at 180 °C about 100 nm. The nanostructures obtained are shown in figure 14. The authors have tried to explain the growth of the nanostructures with the schematic diagram shown in figure 15.

CTAB being a cationic surfactant reduces the surface tension and as such inhibits the formation of a new phase. CTAB acts as a transport medium to transport $Zn(OH)_4^{2-}$ growth units which come together to form individual rod-like structures at 120 °C which then self-assemble into the ZnO nanoflowers. However, at temperatures of 150 and 180 °C, two-dimensional nanosheets are formed which then self-assemble into the cabbages.

Three-dimensional ZnO nanostructures have also been successfully synthesized through a simple hydrothermal process using ammonia and zinc acetate dihydrate at 95 °C [82]. Different morphologies were observed when the pH of the growth solution was changed between 9 and 11.8. The SEM micrographs are shown in figure 16 and a summary of the results is presented in table 4.

4.4. Hydrothermal synthesis using microwaves

Another method of synthesis of nanostructures which is receiving a lot of interest lately is the use of microwave heating in place of conventional heating. Use of microwaves for synthesis was first reported in 1986 by Gedye *et al* [83] following which there has been an increase in the use of microwaves for nanostructure synthesis [51, 84, 85]. Ma *et al* [86] have synthesized ZnO micro and nanostructures using zinc nitrate hexahydrate and pyridine in a hydrothermal process through microwave irradiation at 90 °C for 10 min. Adjusting the concentration of pyridine in the reaction

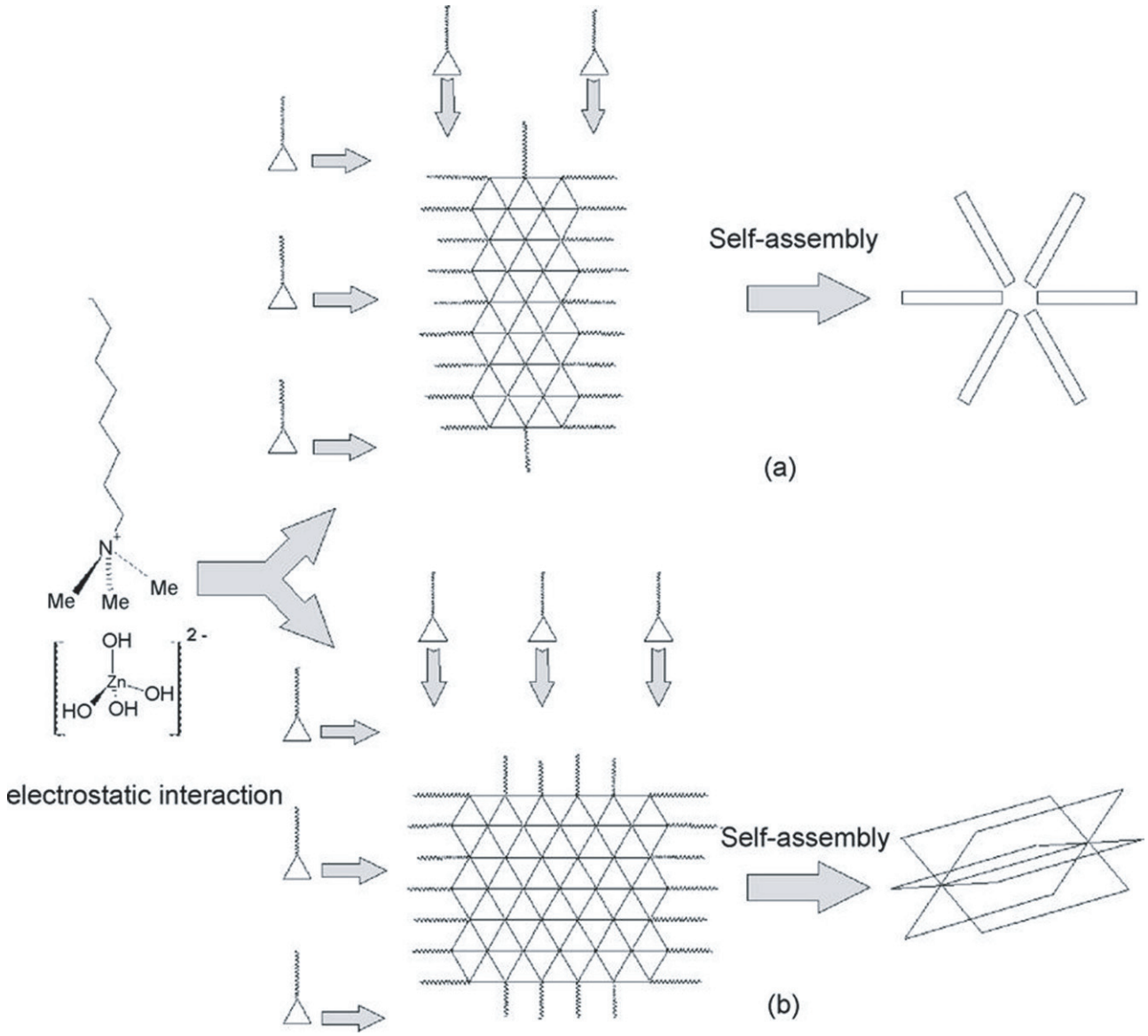

Figure 15. Schematic illustration explaining the growth of ZnO micro and nanostructures synthesized through CTAB-assisted hydrothermal process at different temperatures (a) 120 °C and (b) 150 °C and 180 °C. (Reproduced with permission from [81] © 2008 Elsevier.)

bath, various morphologies of ZnO could be synthesized like hexagonal columns, linked hexagonal needles, hollow structures and hexagonal nanorings. Some of the structures are shown in figure 17.

4.5. Chemical double dip technique

Vijayan *et al* [87] have successfully grown thin films of ZnO using a double dip technique using sodium zincate (Na_2ZnO_2) as the first dipping solution followed by a second dipping in hot water. The conversion of sodium zincate into zinc oxide in presence of water follows the simple reaction

$$Na_2ZnO_2 + H_2O \rightarrow ZnO + 2NaOH. \quad (15)$$

Polycrystalline thin films with high preferential orientation along the (002) plane could be obtained using the double dip technique. The microstructural parameters were dependent upon the temperature of the hot water bath, the pH as well as the amount of $Zn(SO_4)_2$ used for preparing the sodium zincate solution.

5. Crystal structure of hydrothermally grown ZnO nanostructures

The hydrothermally grown ZnO nanostructures are single crystalline and exhibit the wurtzite structure of ZnO. X-ray diffraction (XRD) analyses for different ZnO nanostructures grown through hydrothermal methods revealed the hexagonal wurtzite structure, and the peaks could be indexed according to JCPDS card No. 79-2205 with $a = 0.3249$ nm and $c = 0.5205$ nm [46, 77, 81]. Some of the XRD results are shown in figure 18.

Further structural characterizations can be performed using high resolution transmission electron microscopy (HRTEM). Fast Fourier transforms (FFT) and inverse FFT

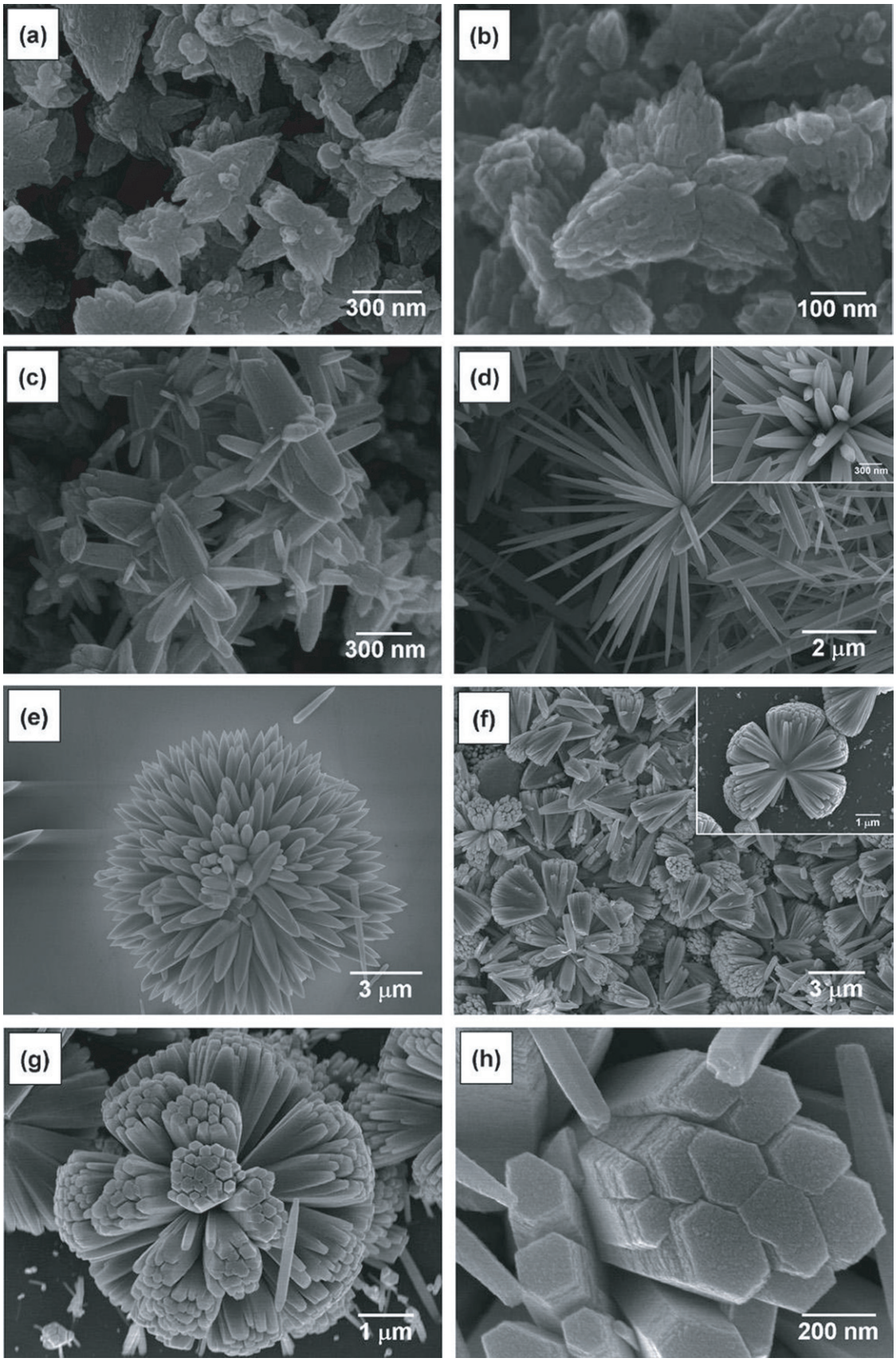

Figure 16. SEM images of the ZnO 3D nanostructures synthesized at different pH: (a) pH 9.0, (b) pH 9.5, (c) pH 10.0, (d) pH 10.5, (e) pH 11.0, (f) pH 11.5, (g) pH 11.8 and (h) magnified image of pH 11.8. (Reproduced with permission from [82] © 2008 Elsevier.)

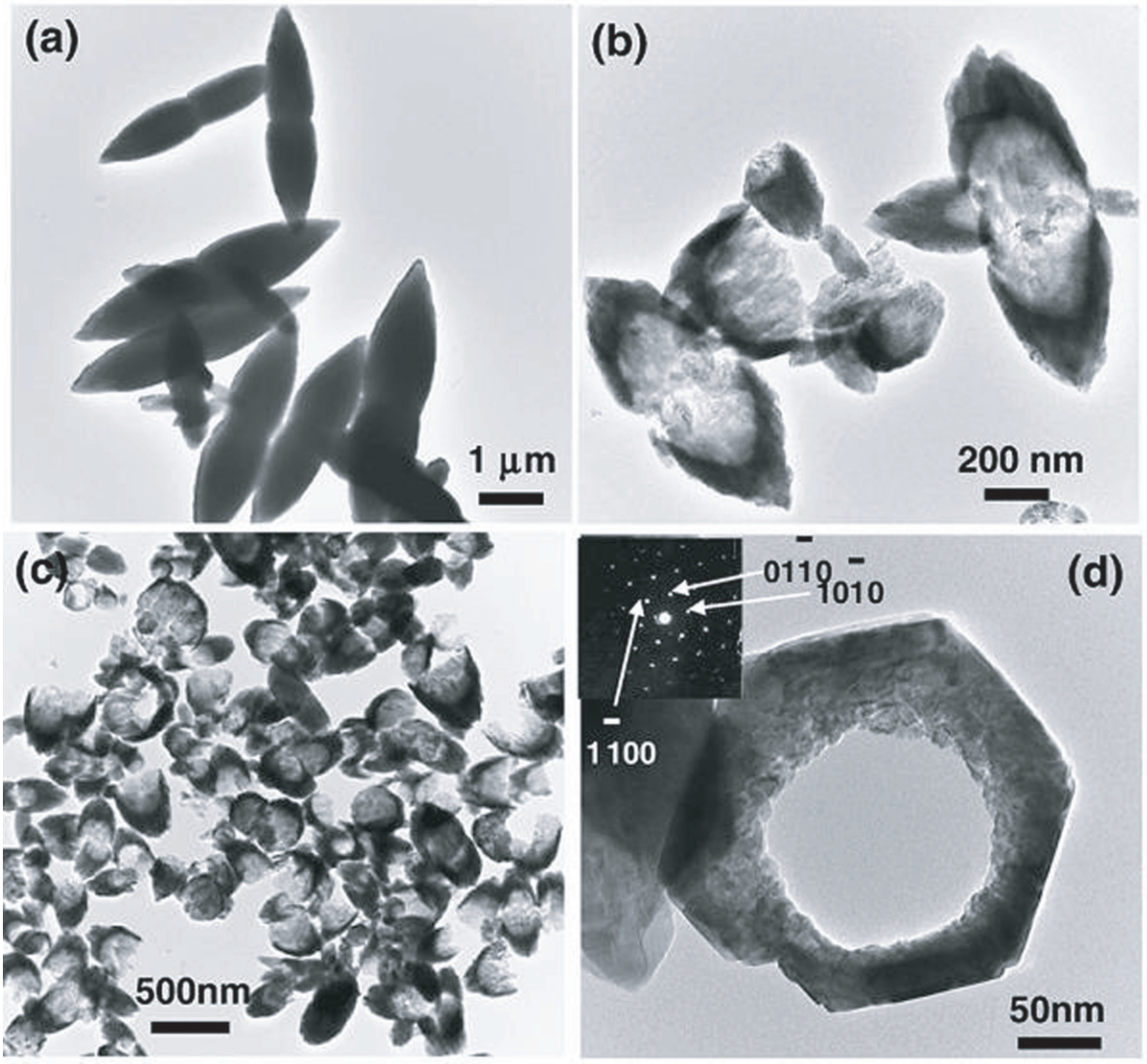

Figure 17. TEM micrographs of the samples synthesized through microwave irradiation in aqueous solution of $Zn(NO_3)_2$ and pyridine at 90 °C for 10 min. (Reproduced with permission from [86] © 2007 Elsevier.)

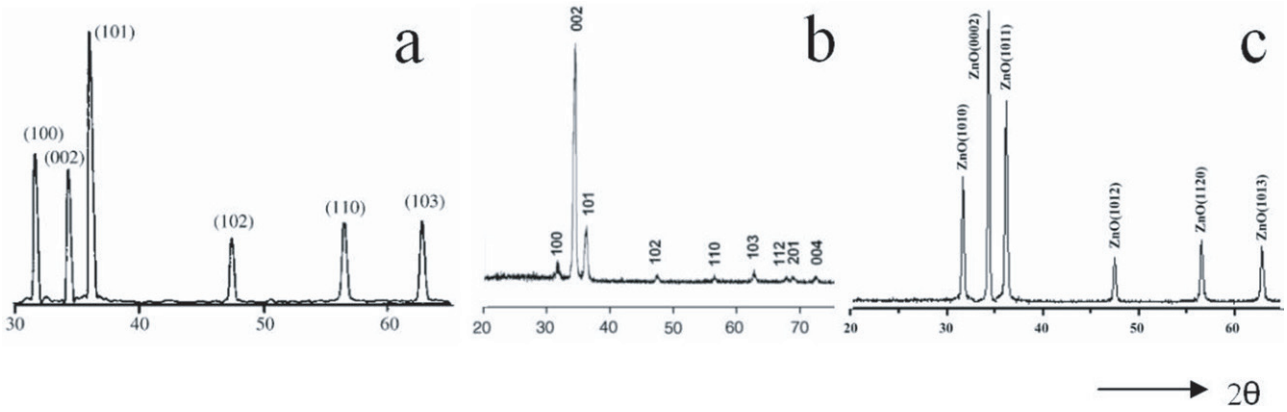

Figure 18. Typical x-ray diffraction (XRD) patterns for different ZnO nanostructures prepared using hydrothermal methods (a) nanoparticles, (b) nanorods and (c) nanoflowers. The indexed peaks correspond to the hexagonal wurtzite structure [46, 80, 81]. (Reproduced with permission from [46] © 2006 Elsevier, [79] © 2007 Elsevier and [80] © 2007 Elsevier.)

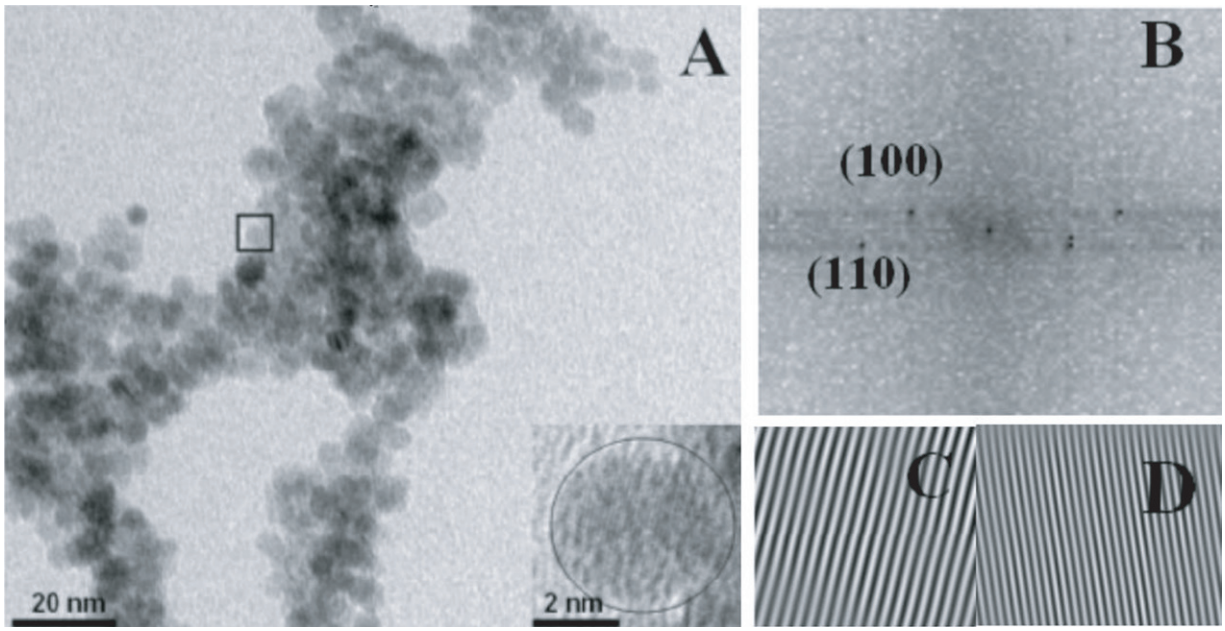

Figure 19. (A) High resolution TEM image of ZnO nanoparticles (inset: magnification of the squared area.) (B) Fast Fourier transform done on the squared area (C), (D) Inverse fast Fourier transform of (B). (Reproduced with permission from Baruah *et al* [51].)

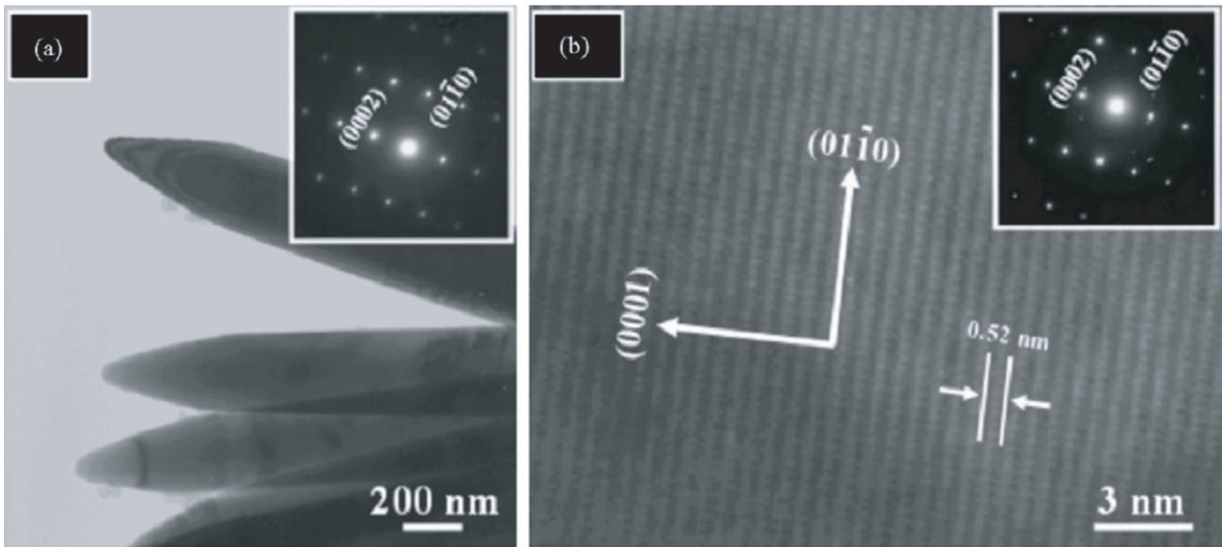

Figure 20. (a) Low resolution TEM image (inset: SAED pattern). (b) High resolution TEM image showing lattice fringes (inset: SAED pattern). (reproduced with permission from [79] © 2007 Elsevier.)

of HRTEM images of ZnO nanoparticles [51] confirmed the wurtzite structure. One of the imaged particles is shown in figure 19(B) and the corresponding FFT and Inverse FFTs are shown in figures 19(C)–(E). Lattice spacings of 0.28 nm and 0.16 nm indicate the presence of the (100) and (110) planes.

Another method of confirming the crystal structure is through the use of selected area electron diffraction (SAED) setup which comes as an accessory with TEMs. The SAED pattern for ZnO nanorods synthesized through a hydrothermal method [79] is shown in figure 20 along with low and high magnification TEM images. Figure 20(a) shows a low resolution TEM image of pointed tip ZnO nanorods. The corresponding SAED pattern (inset) confirmed that the rods are single crystalline and grew along the [0001] direction.

The lattice fringe spacing in the HRTEM image is 0.52 nm which corresponds to the hexagonal wurtzite structure of ZnO and indicates that the growth occurred along the [0001] direction. The SAED pattern (inset) agrees with the HRTEM observation [79].

6. Doping of ZnO nanostructures through hydrothermal routes

Doping of semiconducting nanostructured materials is the primary technique for controlling properties like bandgap, electrical conductivity and ferromagnetism. Transition metal doping of II–VI and III–V semiconductors is generating a lot of interest from researchers for possible applications in

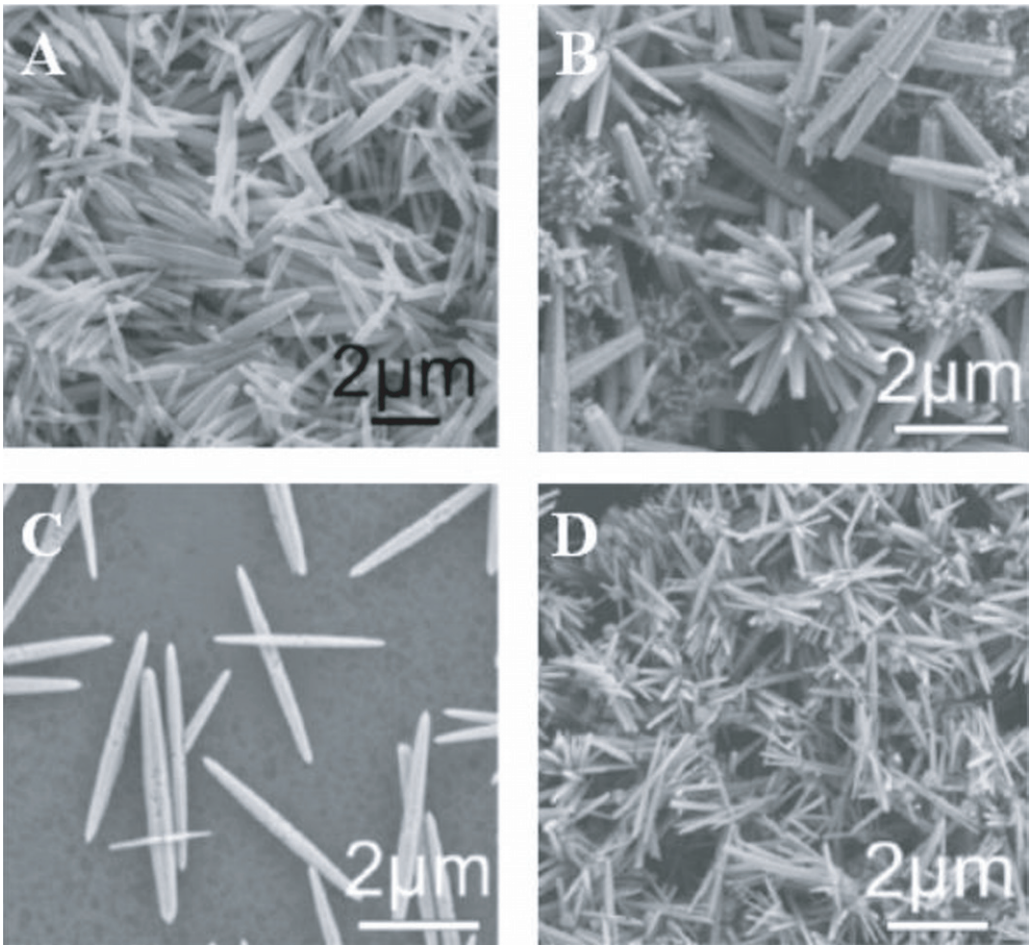

Figure 21. SEM images of ZnO nanorods grown hydrothermally (A) undoped (B) doped using 10% Co solution (C) doped using 10% Co Cr solution and (D) doped using 10% Mn solution. (Reproduced with permission from [99] © 2007 Elsevier.)

spintronics and visible light photocatalysis. A lot of work has been done in the area of transition metal doping of ZnO single crystals and thin films [88–92]. However, a few reports on the synthesis and characterization of ZnO nanostructures doped with different impurities like Al, Sn, Ga, In, Sb, Cu, etc are available in the literature [93–98]. Li *et al* [99] has synthesized ZnO nanorods doped with manganese (Mn), chromium (Cr) and cobalt (Co) in a hydrothermal synthesis using zinc nitrate, transition metal nitrate and hexamethylenetetramine. It was observed that the doping was good with Mn (8% doping from a 10% solution) and Co (17% doping from a 10% solution) dopants and poor with Cr (4% doping from a 10% solution). The morphology of the doped ZnO nanorods was different from that of the undoped nanorods, the SEM images of which are shown in figure 21.

Yuhas *et al* [100] has communicated the successful doping of ZnO nanorods with Co by the thermal decomposition of zinc acetate and cobalt (II) acetate in refluxing trioctylamine. The reaction temperature was set at 310 °C and the reaction was allowed to continue from 45 to 180 min to obtain rods of different diameters. The hydrothermal synthesis of Al-doped ZnO nanopowders was reported by Piticescu *et al* [101]. The synthesis was carried out in a 2L computer-controlled Teflon autoclave using KOH as a mineralizing agent. Indium doping of ZnO nanorods was done after the rods were grown hydrothermally through a post deposition thermal annealing in an inert atmosphere [102]. Indium doping during the hydrothermal synthesis could not be carried out due to the formation of $In(OH)_3$ phase. Doping was carried out successfully for 0.5, 1 and 2%.

7. Conclusion

Hydrothermal synthesis of ZnO nanostructures is simple and efficient and it is receiving a lot of attention of late. Various additives are used in aqueous medium to successfully synthesize ZnO nanostructures of different morphologies, a mixture of zinc nitrate and hexamine are the most popular. ZnO nanostructures are attractive candidates for applications in a host of devices like solar cells, sensors, detectors, energy generators as well as artificial structures for tissue engineering. ZnO nanostructures are being increasingly used as photocatalysts for degrading harmful contaminants like pesticides from ground water. Within the next decade, ZnO nanostructures are most likely to move into industrial applications.

Acknowledgments

The authors would like to acknowledge partial financial support from the National Nanotechnology Center, belonging to the National Science and Technology Development Agency (NSTDA), Ministry of Science and Technology (MOST), Thailand and the Centre of Excellence in Nanotechnology at the Asian Institute of Technology.

Reference

[1] Emanetoglu N W, Gorla C, Liu Y, Liang S and Lu Y 1999 *Mater. Sci. Semicond. Process* **2** 247
[2] Chen Y, Bagnall D and Yao T 2000 *Mater. Sci. Eng.* B **75** 190
[3] Liang S, Sheng H, Liu Y, Hio Z, Lu Y and Chen H 2001 *J. Cryst. Growth* **225** 110
[4] Saito N, Haneda H, Sekiguchi T, Ohashi N, Sakaguchi I and Koumoto K 2002 *Adv. Mater.* **14** 418
[5] Lee J Y, Choi Y S, Kim J H, Park M O and Im S 2002 *Thin Solid Films* **403** 533
[6] Mitra A, Chatterjee A P and Maiti H S 1998 *Mater. Lett.* **35** 33
[7] Koch M H, Timbrell P Y and Lamb R N 1995 *Semicond. Sci. Technol.* **10** 1523
[8] Gratzel M 2005 *MRS Bull.* **30** 39374
[9] Baxter J B, Walker A M, van Ommering K and Aydil E S 2006 *Nanotechnology* **17** S304
[10] Lin Y, Zhang Z, Tang Z, Yuan F and Li J 1999 *Adv. Mater. Opt. Electron.* **9** 205
[11] Padmavathy N and Vijayaraghavan R 2008 *Sci. Technol. Adv. Mater.* **9** 035004
[12] Iijima S 1991 *Nature* **354** 56
[13] Cui Y, Lauhon L J and Gudiksen M S 2001 *Appl. Phys. Lett.* **78** 2214
[14] Burghard G M, Kim G T, Dusberg G S, Chiu P W, Krstic V, Roth S and Han W Q 2001 *J. Appl. Phys.* **90** 5747
[15] Duan X, Huang Y, Cui Y, Wang J and Lieber C M 2001 *Nature* **409** 66
[16] Bai Z G, Yu D P, Zhang H Z, Ding Y, Gai S Q, Hang X Z, Hiong Q L and Feng G C 1999 *Chem. Phys. Lett.* **303** 311
[17] Huang M H, Wu Y, Feick H, Tran N, Webe E and Yang P 2001 *Adv. Mater.* **13** 113
[18] Huang M H, Mao S, Feick H, Yan H, Wu Y, Kind H, Weber E, Russo R and Yang P 2001 *Science* **292** 1897
[19] Shi G, Mo C M, Cai W L and Zhang L D 2005 *Solid State Commun.* **115** 253
[20] Baruah S, Thanachayanont C and Dutta J 2008 *Sci. Technol. Adv. Mater.* **9** 025009
[21] Huang Y, Zhang Y, Bai X, He J, Liu J and Zhang X 2006 *J. Nanosci. Nanotechnol.* **6** 2566
[22] Hughes W L and Wang Z L 2005 *Appl. Phys. Lett.* **86** 043106
[23] Kong X Y and Wang Z L 2003 *Nano Lett.* **3** 1625
[24] Hughes W L and Wang Z L 2004 *J. Am. Chem. Soc.* **126** 6703
[25] Sun T, Qiu J and Liang C 2008 *J. Phys. Chem.* C **112** 715
[26] Snure M and Tiwari A 2007 *J. Nanosci. Nanotechnol.* **7** 485
[27] Wang Z L 2004 *J. Phys.: Condens. Matter* **16** R829
[28] Spanhel L 2006 *J. Sol–Gel Sci. Technol.* **39** 7
[29] Ma X, Zhang H, Ji Y, Xu J and Yang D 2005 *Mater. Lett.* **59** 3393
[30] Kohls M, Bonnani M and Spanhel L 2002 *Appl. Phys. Lett.* **81** 3858
[31] Xu H Y, Wang H, Zhang Y C, Wang S, Zhu M and Yan H 2003 *Cryst. Res. Technol.* **38** 429
[32] Shingubara S 2003 *J. Nanoparticle Res.* **5** 17
[33] Krunks M and Mellikov E 1995 *Thin Solid Films* **270** 33
[34] Ayouchi R, Martin F, Leinen D and Ramos-Barrado J R 2003 *J. Cryst. Growth* **247** 497
[35] Wang Y C, Leu I C, Chung Y W and Hon M H 2006 *Nanotechnology* **17** 4445
[36] Tang C C, Fan S S, Lamy de la, Chapelle M and Li P 2001 *Chem. Phys. Lett.* **333** 12
[37] Pan Z W, Dai Z R and Wang Z L 2001 *Science* **291** 1947
[38] Wang Z and Li H L 2002 *Appl. Phys.* A **74** 201
[39] Miao L, Ieda Y, Tanemura S, Cao Y G, Tanemura M, Hayashi Y, Toh S and Kaneko K 2007 *Sci. Technol. Adv. Mater.* **8** 443
[40] Dalal S H, Baptista D L, Teo K B K, Lacerda R G, Jefferson D A and Milne W I 2006 *Nanotechnology* **17** 4811
[41] Satoh Y, Ohshio S and Saitoh H 2005 *Sci. Technol. Adv. Mater.* **6** 215
[42] Yasuda T and Segawa Y 2004 *Phys. Status Solidi* b **241** 676
[43] Li Z W and Gao W 2007 *Thin Solid Films* **515** 3323
[44] Lagashetty A, Havanoor V, Basavaraja S, Balaji S D and Venkataraman A 2007 *Sci. Technol. Adv. Mater.* **8** 484
[45] Tokumoto M, Briois V, Santili C V and Pulcinelli S H 2003 *J. Sol–Gel Sci. Technol.* **26** 547
[46] Baruwati B, Kumar D K and Manorama S V 2006 *Sensors Actuators* B **119** 676
[47] Lu C H and Yeh C H 2000 *Ceram. Int.* **26** 351
[48] Chen D, Jiao X and Cheng G 2000 *Solid State Commun.* **113** 363
[49] Musić S, Popović S, Maljković M and Dragčević D 2002 *J. Alloys Compd.* **347** 324
[50] Vishwanathan R and Gupta R B 2003 *J. Supercritical Fluids* **27** 187
[51] Baruah S, Rafique R F and Dutta J 2008 *Nano* at press
[52] Andres-Vergés M, Mifsud A and Serna C J 1990 *J. Chem. Soc. Faraday Trans.* **86** 959
[53] Vayssieres L, Keis K and Lindquist S E 2001 *J. Phys. Chem.* B **105** 3350
[54] Schmidt-Mende L and MacManus-Driscoll J L 2007 *Mater. Today* **10** 40
[55] Ashfold M N R, Doherty R P, Ndifor-Angwafor N G, Riley D J and Sun Y 2007 *Thin Solid Films* **515** 8679
[56] Govender K, Boyle D S, Kenway P B and O'Brien P 2004 *J. Mater. Chem.* **14** 2575
[57] Sugunan A, Warad H C, Boman M and Dutta J 2006 *J. Sol–Gel Sci. Technol.* **39** 49
[58] Vayssieres L, Keis K, Lindquist S E and Hagfeldt A 2001 *J. Phys. Chem.* B **105** 3350
[59] Vayssieres L 2003 *Adv. Mater.* **15** 464
[60] Sun Y, Riley D J and Ashfold M N R 2006 *J. Phys. Chem.* B **110** 15186
[61] Tian Z R, Voigt J A, Liu J, Mckenzie B, Mcdermott M J, Rodriguez M A, Konishi H and Xu H 2003 *Nat. Mater.* **2** 821
[62] Pal U and Santiago P 2005 *J. Phys. Chem.* B **109** 15317
[63] Tang L, Bao X-B, Zhou H and Yuan A-H 2008 *Physica* E **40** 924
[64] Li F, Hu L, Li Z and Huang X 2007 *J. Alloys Compd.* **465** L14
[65] Zhang X Y, Dai J Y, Ong H C, Wang N, Chan H L W and Choy C L 2004 *Chem. Phys. Lett.* **393** 17
[66] Chen Y, Yu R, Shi Q, Qin J and Zheng F 2007 *Mater. Lett.* **61** 4438
[67] Ni Y H, Wei X-W, Ma X and Hong J-M 2005 *J. Cryst. Growth* **283** 48
[68] Zhao D Y, Feng J L, Huo Q S, Melosh N, Fredrickson G H, Chmelka B F and Stucky G D 1998 *Science* **279** 548
[69] Yang P D, Deng T, Zhao D Y, Feng P Y, Pine D, Chmelka B F, Whitesides G M and Stucky G D 1998 *Science* **282** 2244
[70] Melosh N A, Davidson P and Chmelka B F 2000 *J. Am. Chem. Soc.* **122** 823
[71] Yu C Z, Tian B, Fan J, Stucky G D and Zhao D Y 2002 *J. Am. Chem. Soc.* **124** 4556
[72] Zhang R, Liu J, Han B X, He J, Liu Z M and Zhang J L 2003 *Langmuir* **19** 8611

[73] Zhang Z and Mu J 2007 *J. Colloid Interface Sci.* **307** 79
[74] Peterson R B, Fields C L and Gregg B A 2004 *Langmuir* **20** 5114
[75] Wang Z, Qian X-F, Yin J and Zhu Z-K 2004 *J. Solid State Chem.* **177** 2148
[76] Li W J, Shi E W, Zhong W Z and Yin Z W 1999 *J. Cryst. Growth* **203** 186
[77] Zhang J, Sun L D, Yin J L, Su H L, Liao C S and Yan C H 2002 *Chem. Mater.* **14** 4172
[78] Li Z, Huang X, Liu J, Li Y, Ji X and Li G 2007 *Mater. Lett.* **61** 4362
[79] Wahab R, Ansari S G, Kim Y S, Seo H K, Kim G S, Khang G and Shin H-S 2007 *Mater. Res. Bull.* **42** 1640
[80] Shao S, Jia P, Liu S and Bai W 2008 *Mater. Lett.* **62** 1200
[81] Li F, Hu L, Li Z and Huang X 2008 *J. Alloys Compd.* **465** L14
[82] Jang J M, Kim S D, Choi H M, Kim J Y and Jung W G 2008 *Mater. Chem. Phys.* doi:10.1016/j.matchemphys.2008.07.108
[83] Gedye R, Smith F, Westaway K, Humera A, Baldisera L, Laberge L and Rousell L 1986 *Tetrahedron Lett.* **27** 279
[84] Zhu Y J, Wang W W, Qi R J and Hu X L 2004 *Angew. Chem., Int. Ed. Engl.* **43** 1410
[85] Tsuji M, Hashimoto M, Nishizawa Y, Kubokawa M and Tsuji T 2005 *Chem. Eur. J.* **11** 440
[86] Ma M-G, Zhu Y J, Cheng G F and Huang Y H 2007 *Mater. Lett.* **62** 507
[87] Vijayan T A, Chandramohan R, Valanarasu S, Thirumalai J, Venkateswaran S, Mahalingam T and Srkumar S R 2008 *Sci. Technol. Adv. Mater.* **9** 035007
[88] Jung S W, An S-J, Yi G C, Jung C U, Lee S-I and Cho S 2002 *Appl. Phys. Lett.* **80** 4561
[89] Cheng X M and Chien C L 2003 *J. Appl. Phys.* **93** 7876
[90] Yoon S W, Cho S-B, We S C, Yoon S, Suh B J, Song H K and Shin Y J 2003 *J. Appl. Phys.* **93** 7879
[91] Fukumura T, Jin Z, Kawasaki M, Shono T, Hasegawa T and Koinuma H 2001 *Appl. Phys. Lett.* **78** 958
[92] Robers B K, Pakhomov A B, Shutthanandan V S and Krishnan K M 2005 *J. Appl. Phys.* **97** 10D310
[93] Bae S Y, Na C W, Kang J H and Part J 2005 *J. Phys. Chem.* B **109** 2526
[94] Cimitan S, Albonetti S, Forni L, Peri F and Lazzari D 2009 *J. Colloid Interface Sci.* **329** 73
[95] Majumder S B, Jain M, Dobal P S and Katiyar R S 2003 *Mater. Sci. Eng.* B **103** 16
[96] Xu C, Kim M, Chun J and Kim D 2005 *Appl. Phys. Lett.* **86** 133107
[97] Zuo J, Xu C, Zhang L, Xu B and Wu R 2001 *J. Raman Spectrosc.* **32** 979
[98] Agne T, Guan Z, Li X M, Wolf H, Wichert T, Natter H and Hempelmann R 2003 *Appl. Phys. Lett.* **83** 1204
[99] Li D, Liu Z T, Leung Y H, Djurisic A B, Xie M H and Chan W K 2008 *J. Phys. Chem. Solids* **69** 616
[100] Yuhas B D, Zitoun D O, Pauzauskie P J, He R and Yang P 2006 *Angew. Chem., Intl. Ed. Engl.* **45** 420
[101] Piticescu R R, Piticescu R M and Monty C J 2006 *J. Eur. Ceram. Soc.* **26** 2979
[102] Morales A E, Zaldivar M H and Pal U 2006 *Opt. Mater.* **29** 100